Tumor Fibroblast Specific Activation of a Hybrid Ferritin Nanocage-Based Optical Probe for Tumor Microenvironment Imaging

Tianjiao Ji, Ying Zhao, Jing Wang, Xin Zheng, Yanhua Tian, Yuliang Zhao, and Guangjun Nie**

During various phases of tumor progression, such as degradation of the extracellular matrix (ECM), angiogenesis, tumor invasion, and metastasis, secretion of specific enzymes plays crucial roles during these disease processes in tumor microenvironment.[1,2] These specific enzymes are therefore attractive targets for both tumor therapy and imaging.[3] Our previous studies have shown that inhibition of both expression and activity of matrix metalloproteinases (MMPs) can significantly prevent malignant tumor invasion and metastasis via the prison the tumor cell strategy, in which degradation of ECM was dramatically decreased after the metallofullerene nanoparticles treatment.[4–6] For clinical diagnostics perspective, to examine the exact site of tumors and the expression degree of these enzymes are particularly valuable. To meet the urgent demand for bioimaging in live systems, continuous efforts are required for developing intelligent and sensitive imaging probes, and the applications of functional nanomaterials may provide enormous opportunity. Some novel enzyme-responsive nanoprobes have been developed to image and monitor the abnormal expression of these enzymes in tumor tissue, where the activity of an enzyme elicited a specific response via the nanoparticle assembly-disassembly process to produce an activity-depending signal.[7–9] Enzymes that have attracted much recent attention as candidate targets for nanoprobes involve caspase-3,[10,11] urokinase plasminogen activator (uPA),[12] and MMPs.[13,14] Despite progress achieved, further improvements are still required regarding design of novel nanoprobes with enhanced efficiency and specificity, as the enzymes currently used may not be the most abundant and potent enzymes with lack of tumor type specificity. Among various cells present in tumor tissues, it is likely that enzymes expressed by the greatly abundant stromal cells will be increasingly noticed in the near future as efficient and specific new targets and may provide important insights into cancer biology.[15]

Fibroblast activation protein-α (FAP-α), a membrane-bound serine protease, is highly and specifically expressed by cancer-associated fibroblasts (CAFs) and pericytes in epithelial tumors, without any notable expression in normal adult tissues.[16–18] FAP-α exhibits both dipeptidyl peptidase and collagenase proteolytic activity, being able to cleave N-terminal dipeptides from polypeptides with L-proline or L-alanine in the penultimate position, as well as degrade gelatin and native type I collagen.[16,19–21] Thus, FAP-α plays a critical role in shaping the microenvironment to promote tumor growth and invasion through degrading ECM.[22–24] Although the biological function of FAP-α still needs further study, the specific expression and the unique enzymatic activity of FAP-α make it a potentially attractive therapeutic and diagnostic target in the tumor microenvironment.[25] The tumor growth and invasion can be inhibited by suppressing the activity of FAP-α.[25,26] However, the diagnosis value of FAP-α has not been exploited as a specific biomarker to precisely diagnose FAP-α positive tumors and follow the prognosis. Moreover, FAP-α-positive stromal cells compose the most abundant tumor stromal components.[20,27] In the tumor microenvironment, FAP-α-positive stromal cells dominantly surround the tumor-derived vascular endothelial cells,[28] further facilitating the efficient and specific accumulation and activation of the FAP-α-responsive nanoprobes.

In this study, we designed a ferritin-based FAP-α-responsive fluorescence probe for CAFs positive carcinoma imaging. Unlike tumor cell-targeting probes, which need to reach a certain depth into tumor tissue to interact with tumor cells, the ferritin-based probe could be activated immediately (about 0.5 h after injection) as they penetrate the tumor blood vessels and come across the FAP-α molecules on the membrane of CAFs in the tumor microenvironment (**Scheme 1**). Hybrid ferritin has well been developed as an approach to build multi-functional nanoparticles for protein-based nanoprobe construction.[29–31] Ferritin is a family of proteins consisting of 24 subunits that exist in many types of organisms. As a type of stable cage-like biomolecules circulated in blood, ferritin-based nanomaterials are supposed to possess good biocompatibility and sufficient stability. Furthermore, its interior cavity for biomineralization and exterior

T. Ji, Prof. Y. Zhao, Prof. J. Wang, X. Zheng, Y. Tian, Y. Zhao, Prof. G. Nie
Chinese Academy of Sciences Key Laboratory for Biomedical Effects of Nanomaterials and Nanosafety, National Center for Nanoscience and Technology, China, Beijing 100190, China
E-mail:zhaoying@nanoctr.cn; niegj@nanoctr.cn

DOI: 10.1002/smll.201300600

© 2013 Wiley-VCH Verlag GmbH & Co. KGaA, Weinheim

Petitioner GE Healthcare – Ex. 1045, p. 2427

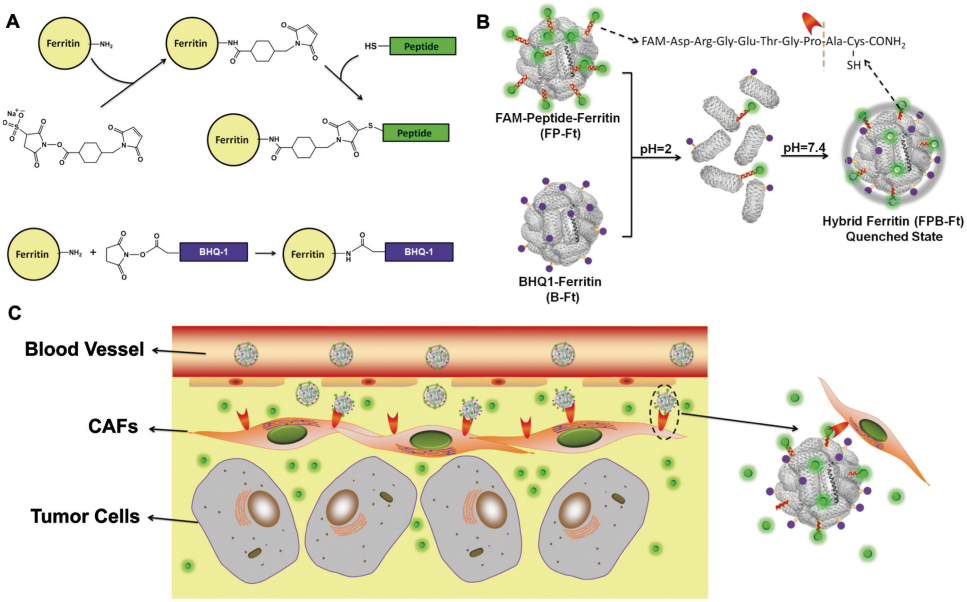

Scheme 1. The schematic illustration of the ferritin-based CAFs-responsive fluorescence nanoprobe (FPB-Ft). A) Design, synthesis and B) assembly of hybrid ferritins and the FPB-Ft; C) the CAFs-dependent activation mechanism of the FPB-Ft fluorescence probe in the tumor microenvironment.

surface for further functionalization endeavor ferritins as the ideal molecules to form multifunctional nanostructures.[29,30] Moreover, the formation and dissociation of the cage-like nano-sized structure of single ferritin molecule is subject to be regulated by the environmental pH. It has been observed that in strong acidic environments (pH = 2.0) the ferritin cage would disassemble into discrete subunits, while at pH = 7.4 these subunits once again self-assemble through non-covalent interactions and restore the cage-like structure.[29–31] This unique pH-responsive architecture has rendered it especially convenient to build multi-functional hybrid ferritins by conjugating different small molecules onto the subunits. Here, we constructed a series of hybrid ferritin fluorescence probes by coupling a fluorescence-tagged peptide that can be specifically cleaved by FAP-α on ferritin subunits, followed by reassembly them under physiological conditions. Considering these favorable properties, our design is making full use of the good biocompatibility and longer half-life of ferritins in the blood circulation; we finally achieved fluorescence imaging in vivo by intravenously injecting this nanoprobe into mice.[32,33] This strategy exhibited high specificity and stimuli-responsive sensitivity in the tumor microenvironment. Based on the results, this novel nanoprobe could be further developed as a promising nanomaterial for tumor microenvironment imaging and tumor diagnosis.

Construction of the hybrid ferritin was carried out according to the procedure shown in Scheme 1A,B. A designed carboxyfluorescein-tagged (FAM-tagged) peptide (FAM-DRGETGPAC, MW 1262) that can be specifically cleaved by FAP-α at the amide bond between Pro and Ala (resulting a fluorescent fragment FAM-DRGETGP, MW 1088) was coupled onto horse spleen ferritins to create the first set of functionalized ferritin, FAM-peptide-ferritin (FP-Ft); meanwhile a second set of functionalized ferritin, black hole quencher (BHQ) linked ferritin, BHQ-ferritin (B-Ft), was prepared by modifying the protein with a fluorescence quencher, BHQ-1. Both sets of ferritins maintained the cage structure after modification, which was confirmed by their morphologies under transmission electron microscopy (TEM), as shown in **Figure 1**A,B. The two sets of ferritins were then mixed and broke down into subunits at pH 2.0, followed by retuning the pH back to neutral (pH 7.4) to allow the reassembly of ferritin particles.[29–31] During the reassembling process, the two sets of subunits hybridized to form the optimal hybrid ferritin (FPB-Ft, FP/B = 1:2),

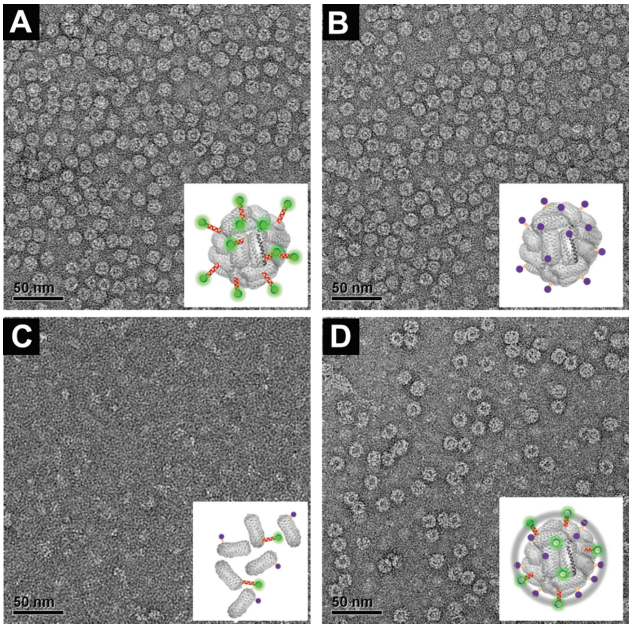

Figure 1. The morphology of ferritins during the process of synthesis. TEM images of the assemblies of A) FP-Ft and B) B-Ft at pH 7.4; C) the disassembled subunits of FP-Ft and B-Ft at pH 2.0, and D) the reassemblies of the hybrid ferritin (FPB-Ft) formed by adjusting the acidic solution back to pH 7.4.

© 2013 Wiley-VCH Verlag GmbH & Co. KGaA, Weinheim

16136829, 2013, 14, Downloaded from https://onlinelibrary.wiley.com/doi/10.1002/smll.201300600 by Jeff Kushan - <Shibboleth>-member@gwu.edu , Wiley Online Library on [12/03/2025]. See the Terms and Conditions (https://onlinelibrary.wiley.com/terms-and-conditions) on Wiley Online Library for rules of use; OA articles are governed by the applicable Creative Commons License

Petitioner GE Healthcare – Ex. 1045, p. 2428

small

i.e., the designed fluorescence quenched nanoprobe, as showed in Figure 1C,D. As a fluorescence resonance energy transfer (FRET) quencher,[34,35] BHQ-1 quenched the fluorescence of nearby fluorescence-tagged peptide, hence the nanoprobe was at a quiescent stage until activated by encountering with FAP-α. This enzyme triggered activation would significantly improve both the sensitivity and specificity for optical imaging. The fluorescent peptide, FAM-DRGETGPAC, has been demonstrated as being selective for FAP-α even after the conjugation with ferritins, which was validated by mass spectrometric analysis (Figure S1 in the Supporting Information). When FAP-α was added into free FAM-tagged peptide, the peptide peak at m/z = 1263 disappeared and the peak m/z = 1089 corresponding to the fluorescence fragment FAM-DRGETGP emerged, 5 h after the treatment; and in the case of FP-Ft, the peak of m/z = 1263 was not present in mass spectrum due to chemical binding between the peptide and ferritin, while the peak m/z = 1089 was observed after the addition of FAP-α, indicating the releasing of the same fragment. It could thus be concluded that the FAM-tagged peptide was successfully linked to ferritins and the peptide could be cleaved as desired from ferritins by FAP-α. Details of peptide and BHQ-1 coupling, purification procedures and HPLC analysis can be found in the Supporting Information (Supporting Information Figure S2).

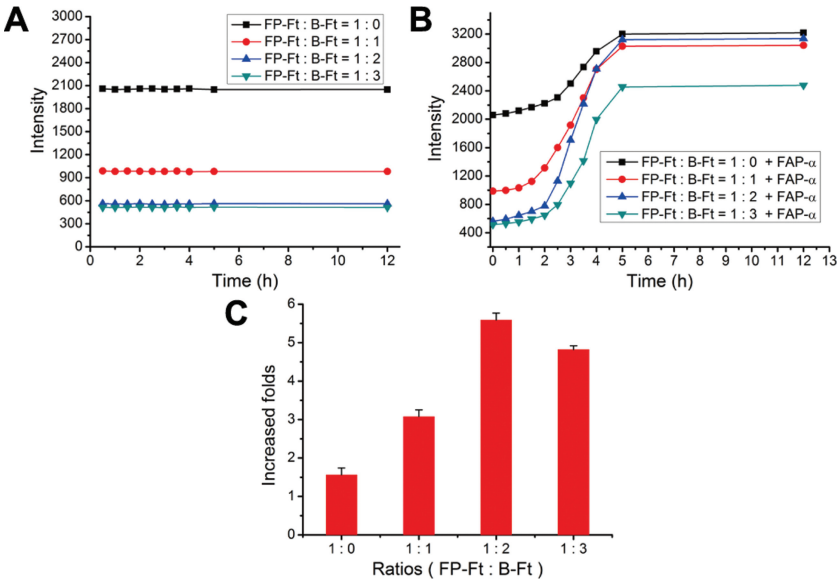

Figure 2. Kinetic changes of the fluorescence intensity of hybrid ferritin with different FP/B ferritin ratios. A) In the absence of FAP-α, the probes could not be activated. B) In the presence of FAP-α, the probes were activated and the fluorescence intensity increased gradually with time. C) Activation capacities of the different hybrid ferritin formulas (with different FP/B ferritin ratios) derived from (A) and (B).

To evaluate the efficiency of such quench/restore approach and to determine the optimal composition of nanoprobe, we prepared hybrid ferritins (1 mg/mL) solutions with different FP/B subunits ratios (1:0, 1:1, 1:2, and 1:3) as substrates, which were then mixed with 0.2 μg/mL FAP-α, respectively. For each ferritin hybrid, stability was tested in the same condition as mentioned above, but with no FAP-α added. Fluorescence intensity of each solution was measured by a fluorescence spectrometer (excitation at 494 nm, emission at 520 nm) every 0.5 h. None of the controls has demonstrated to have any significant change in fluorescence intensity in the 12 h interval (**Figure 2**A), indicating that the nanoprobes could not self-activate spontaneously and remained in stable stage. However, for all the four enzyme-substrate mixtures, the fluorescence intensity increased gradually after the addition of FAP-α and subsequently reached maximum in 5 h, suggesting that the activation of nanoprobes by FAP-α and the activation started as long as FAP-α was added (Figure 2B). When analyzed by mass spectrometry, the peak m/z = 1089 was present in the spectra of all the mixtures after reaction. Among the four ratios, the hybrid ferritins with the ratio of FP/B 1:2 exhibited both the highest quenching efficiency and the optimal fluorescence emission, with a 6-fold increase in fluorescence between the activation state and the quenched state (Figure 2B,C). Increase in FB-Ft proportion (1:1) decreased quenching efficiency (3-fold), while increase in B-Ft proportion (1:3) led to a weaker fluorescence activation (Figure 2C). Therefore, the hybrid ferritin with FP/B 1:2 was used as the optimal nanoprobe during further in vitro experiment, whose fluorescence intensity was measured both in cells and culture media. Prostate CAF, hTERT immortalized, cell line was analyzed with PCR and agarose gel electrophoresis to confirm that the CAFs indeed express FAP-α. Two pairs of primers (183 bp and 165 bp, primer sequences in the Supporting Information) were designed to investigate the existence of the corresponding mRNA, with positive results showing the expression of FAP-α (Supporting Information Figure S3). The CAFs were then monitored by laser-scanning confocal microscopy (LSCM) at various time points during incubation with the nanoprobes (0.05 mg/mL). The imaging results showed that the nanoprobe was activated in an hour and the fluorescence intensity continuously increased with time in the first 5 h time interval (**Figure 3**A). The intensity at 12 h was approximately the same as at 5 h. Considering that most of fluorescent fragments would widely distribute in the culture medium after being cut off from FPB-Ft, the fluorescent emission of the culture media was also analyzed by fluorescence spectroscopy (Figure 3B,C). The results were consistent with Figure 3A, and the fluorescence intensity of the cell culture medium at 12 h was slightly lower than that at 5 h, possibly because more fragments were taken up by the surrounding CAFs. However, no fluorescence was detected in tumor cells, human prostate cancer cell line (PC-3) in the same condition because the tumor cells do not express FAP-α as reported.[20] These in vitro imaging data provided positive indications of the nanoprobe's capability to target FAP-α-positive stromal cells in the tumor microenvironment in vitro.

The potential application of the FAP-α activatable probes for tumor imaging was further investigated in vivo for FAM signal detection (Maestro in vivo imaging system, excitation

© 2013 Wiley-VCH Verlag GmbH & Co. KGaA, Weinheim

16136829, 2013, 14, Downloaded from https://onlinelibrary.wiley.com/doi/10.1002/smll.201300600 by Jeff Kushan - <Shibboleth>-member@gwu.edu , Wiley Online Library on [12/03/2025]. See the Terms and Conditions (https://onlinelibrary.wiley.com/terms-and-conditions) on Wiley Online Library for rules of use; OA articles are governed by the applicable Creative Commons License

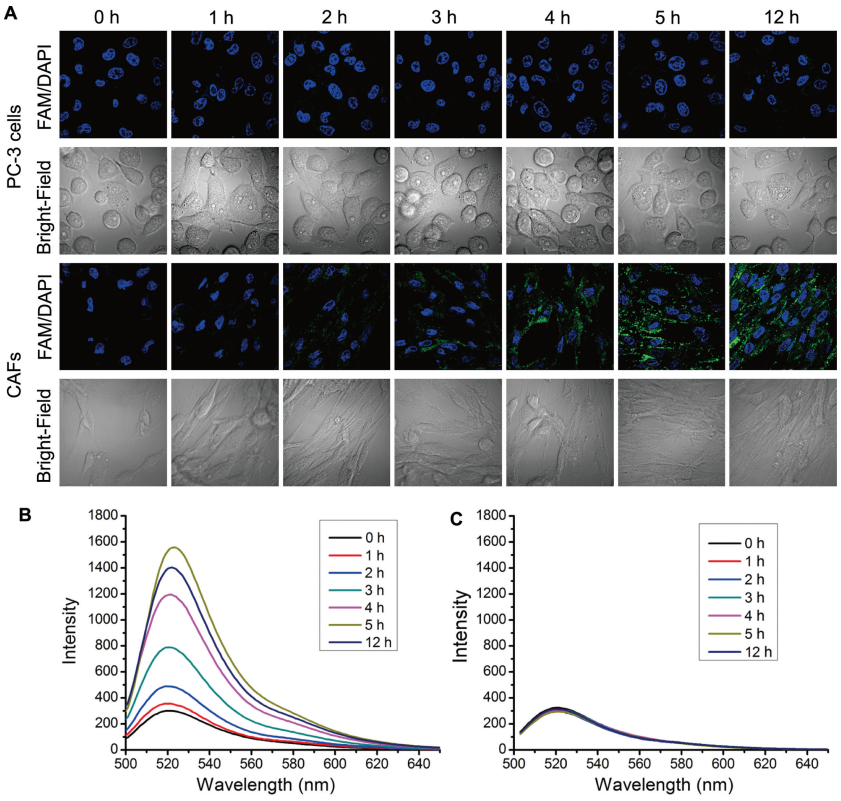

Figure 3. In vitro imaging of the FPB-Ft. The confocal microscopy images of PC-3 cells and CAFs incubated with FPB-Ft probe at various time points. Green and blue fluorescence are FAM and DAPI fluorescence, respectively. The enhanced fluorescence intensity of the culture media at the corresponding time points with (A). B,C) Fluorescence intensity of the CAFs group (B) and the PC-3 group (C).

and emission wavelengths were 490 and 520 nm, respectively). All experiments with mice followed the guidelines for experimental animals and were approved by the local animal welfare committee. One group of BALB/c nude mice (male, 16–18 g body weight) were co-inoculated with 1:1 mixture of PC-3 cells and CAFs (1×10^6 each),[36,37] and another group (PC-3 group) was inoculated with PC-3 cells (2×10^6 each) only. A week later, the diameter of tumors in co-inoculated group grew to 0.5 cm on average, while tumors in the PC-3 group were smaller (0.3 cm) in diameters, which was in accordance with the known promotion effect of CAFs on tumor growth.[22–24] FPB-Ft (150 µL, 0.5 mg/mL in PBS) was intravenously injected into both groups of mice. As expected, the observed FAM signal was largely localized in the co-inoculated group (**Figure 4**A–C), with the intensity reaching its maximum at 1.5 h after injection (Figure 4B). Afterwards the signal decreased gradually, and only a weak signal could be detected in the tumor tissue 5 h after injection, because most fluorescent fragments were metabolized and only a few of them still localized in the tumor site (Figure 4C). Interestingly, no localized signal was observed in the PC-3 group (Figure 4D–F). Two control groups of mice co-inoculated with PC-3 cells and CAFs (1×10^6 each), where the positive control group was treated with FAM-ferritin (F-Ft, with no peptide linked) and the negative control group with FAM-BHQ-ferritin (FB-Ft, no peptide linked, fluorescence quenched), were also investigated. As shown in Supporting Information Figure S5, the positive control group showed a whole body distribution of fluorescence at 1.5 h after injection and the intensity decreased quickly. Only a weak signal could be detected in the tumor after 5 h. No fluorescence signal was observed in the negative control group. These studies suggested that the FPB-Ft reached the tumor through blood circulation and was activated by FAP-α in the co-inoculated group (Scheme 1C), but mainly remained quenched in the PC-3 only group. Ex vivo measurements also exhibited consistent results. The main visceral organs and tumors of both groups were imaged 1.5 h after intravenous injection. In the co-inoculated group, the tumor showed much stronger fluorescence compared to the rather low signal of other organs (except for liver, which showed a detectable signal) (Figure 4G); yet in the PC-3 group, no obvious signal was detected in either the major organs or tumor. Such results implied that the FPB-Ft nanoprobes were only specifically activated by FAP-α in tumors. The possible reason that the PC-3 group had not depicted any targeted signal could be that without CAFs inoculation, and one week tumor inoculation was still not sufficient for the

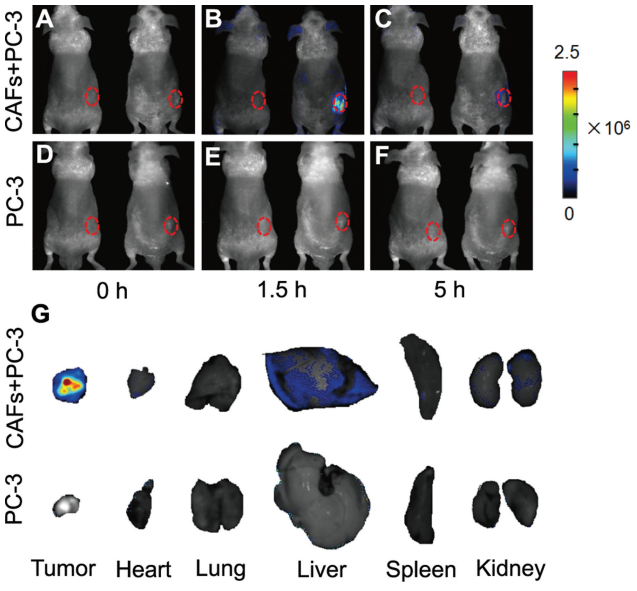

Figure 4. A–F) In vivo and G) ex vivo fluorescence images of the mice injected with FPB-Ft probe. In the co-inoculated group (A–C), the FPB-Ft probe was activated and the FAM signal reached the maximum 1.5 h after FPB-Ft probe injection (B), and the signal could still be observed 5 h after the probe injection (C). In the PC-3 group, no specific signal was detected with time (D–F), showing the FAP-α specific activation of CAFs, but not the tumor cells.

© 2013 Wiley-VCH Verlag GmbH & Co. KGaA, Weinheim

16136829, 2013, 14, Downloaded from https://onlinelibrary.wiley.com/doi/10.1002/smll.201300600 by Jeff Kushan - <Shibboleth>-member@gwu.edu , Wiley Online Library on [12/03/2025]. See the Terms and Conditions (https://onlinelibrary.wiley.com/terms-and-conditions) on Wiley Online Library for rules of use; OA articles are governed by the applicable Creative Commons License

small

tumor cells (PC-3) to recruit or activate the endogenous fibroblasts to become cancer associated fibroblasts in the mice, i.e., not sufficient for the formation of a FAP-α-positive tumor microenvironment.[37,38] Furthermore, although FAP-α is highly specifically expressed in various tumor tissues, it also expressed in granulation tissue and some pathological lesions, such as tissue repair.[39] Special care should be taken to ensure not to include these false-positive observations under such conditions.

In summary, we have reported a ferritin-based fluorescence nanoprobe that was specifically activated by FAP-α expressed in the tumor microenvironment, by which specific fluorescence imaging in vivo was realized through tail vein injection. Owing to abundant and stable FAP-α expression in tumor microenvironment and dominantly surrounding the tumor-derived vascular endothelial cells, there was no need to make the probes reach tumor cells to be activated, likely to result in rapid, specific and sensitive tumor imaging. Our work suggests a promising nanomaterial for tumor imaging through responding to the enzymes of stromal cells in the tumor microenvironment, which may be a new strategy for highly specific and sensitive tumor imaging and diagnosis.

Supporting Information

Supporting Information is available from the Wiley Online Library or from the author.

Acknowledgements

This work was supported by the grants from MOST 973 (2012CB934004, 2010CB933601 and 2012CB932601) and the NSFC (31170962, 51203032, and 21277037).

[1] T. L. Whiteside, *Oncogene* **2008**, *27*, 5904.
[2] R. Majeed, A. Hamid, Y. Qurishi, A. K. Qazi, A. Hussain, M. Ahmed, R. A. Najar, J. A. Bhat, S. K. Singh, A. K. Saxena, *J. Cancer Sci. Ther.* **2012**, *4*, 281.
[3] A. Albini, M. B. Sporn, *Nat. Rev. Cancer* **2007**, *7*, 139.
[4] S. G. Kang, G. Zhou, P. Yang, Y. Liu, B. Sun, T. Huynh, H. Meng, L. Zhao, G. Xing, C. Chen, Y. Zhao, R. Zhou, *Proc. Natl. Acad. Sci. USA* **2012**, *109*, 15431.
[5] H. Meng, G. Xing, B. Sun, F. Zhao, H. Lei, W. Li, Y. Song, Z. Chen, H. Yuan, X. Wang, J. Long, C. Chen, X. Liang, N. Zhang, Z. Chai, Y. Zhao, *ACS Nano* **2010**, *4*, 2773.
[6] H. Meng, G. Xing, E. Blanco, Y. Song, L. Zhao, B. Sun, X. Li, P. C. Wang, A. Korotcov, W. Li, X. J. Liang, C. Chen, H. Yuan, F. Zhao, Z. Chen, T. Sun, Z. Chai, M. Ferrari, Y. Zhao, *Nanomedicine* **2012**, *8*, 136.
[7] H. Koo, M. S. Huh, I. C. Sun, S. H. Yuk, K. Choi, K. Kim, I. C. Kwon, *Acc. Chem. Res.* **2011**, *44*, 1018.
[8] J. Hu, G. Zhang, S. Liu, *Chem. Soc. Rev.* **2012**, *41*, 5933.
[9] A. Razgulin, N. Ma, J. Rao, *Chem. Soc. Rev.* **2011**, *40*, 4186.
[10] Q. D. Nguyen, G. Smith, M. Glaser, M. Perumal, E. Arstad, E. O. Aboagye, *Proc. Natl. Acad. Sci. USA* **2009**, *106*, 16375.
[11] S. H. Choi, I. C. Kwon, K. Y. Hwang, I. S. Kim, H. J. Ahn, *Biomacromolecules* **2011**, *12*, 3099.
[12] Y. Liu, S. Zhou, D. Tu, Z. Chen, M. Huang, H. Zhu, E. Ma, X. Chen, *J. Am. Chem. Soc.* **2012**, *134*, 15083.
[13] T. Zhao, H. Harada, Y. Teramura, S. Tanaka, S. Itasaka, A. Morinibu, K. Shinomiya, Y. Zhu, H. Hanaoka, H. Iwata, H. Saji, M. Hiraoka, *J. Controlled Release* **2010**, *144*, 109.
[14] N. Lee, H. R. Cho, M. H. Oh, S. H. Lee, K. Kim, B. H. Kim, K. Shin, T. Y. Ahn, J. W. Choi, Y. W. Kim, S. H. Choi, T. Hyeon, *J. Am. Chem. Soc.* **2012**, *134*, 10309.
[15] M. J. Bissell, W. C. Hines, *Nat. Med.* **2011**, *17*, 320.
[16] O. Abbas, J. E. Richards, M. Mahalingam, *Mod. Pathol.* **2010**, *23*, 1535.
[17] J. Zhang, J. Liu, *Pharmacol. Ther.* **2013**, *137*, 200.
[18] P. Cirri, P. Chiarugi, *Cancer Metast. Rev.* **2012**, *31*, 195.
[19] S. Aggarwal, W. N. Brennen, T. P. Kole, E. Schneider, O. Topaloglu, M. Yates, R. J. Cotter, S. R. Denmeade, *Biochemistry* **2008**, *47*, 1076.
[20] J. D. Cheng, L. M. Weiner, *Clin. Cancer Res.* **2003**, *9*, 1590.
[21] J. D. Cheng, R. L. Dunbrack Jr, M. Valianou, A. Rogatko, R. K. Alpaugh, L. M. Weiner, *Cancer Res.* **2002**, *62*, 4767.
[22] W. N. Brennen, J. T. Isaaca, S. R. Denmeade, *Mol. Cancer Ther.* **2012**, *11*, 257.
[23] A. Kennedy, H. Dong, D. Chen, W. T. Chen, *Int. J. Cancer* **2009**, *124*, 27.
[24] J. M. Milner, A. Patel, A. D. Rowan, *Arthritis Rheum.* **2008**, *58*, 3644.
[25] A. M. LeBeau, W. N. Brennen, S. Aggarw, S. R. Denmeade, *Mol. Cancer Ther.* **2009**, *8*, 1378.
[26] P. C. Lo, J. Chen, K. Stefflova, M. S. Warren, R. Navab, B. Bandarchi, S. Mullins, M. Tsao, J. D. Cheng, G. Zheng, *J. Med. Chem.* **2009**, *52*, 358.
[27] P. Cirii, P. Chiarugi, *Am. J. Cancer Res.* **2011**, *1*, 482.
[28] J. Li, L. Chen, Z. Qin, *Cancer Microenviron.* **2012**, *5*, 187.
[29] X. Lin, J. Xie, L. Zhu, S. Lee, G. Niu, Y. Ma, K. Kim, X. Chen, *Angew. Chem. Int. Ed.* **2011**, *50*, 1569.
[30] X. Lin, J. Xie, G. Niu, F. Zhang, H. Gao, M. Yang, Q. Quan, M. A. Aronova, G. Zhang, S. Lee, R. Leapman, X. Chen, *Nano Lett.* **2011**, *11*, 814.
[31] K. Li, Z. P. Zhang, M. Luo, X. Yu, Y. Han, H. P. Wei, Z. Q. Cui, X. E. Zhang, *Nanoscale* **2012**, *4*, 188.
[32] J. Fan, J. J. Yin, B. Ning, X. Wu. Y. Hu, M. Ferrari, G. J. Anderson, J. Wei, Y. Zhao, G. Nie, *Biomaterials* **2011**, *32*, 1611.
[33] C. Sun, H. Yang, Y. Yuan, X. Tian, L. Wang, Y. Guo, L. Xu, J. Lei, N. Gao, G. J. Anderson, X. J. Liang, C. Chen, Y. Zhao, G. Nie, *J. Am. Chem. Soc.* **2011**, *133*, 8617.
[34] C. J. Mu, D. A. LaVan, R. S. Langer, B. R. Zetter, *ACS Nano* **2010**, *4*, 1511.
[35] H. Lee, K. Lee, I. K. Kim, T. G. Park, *Biomaterials* **2008**, *29*, 4709.
[36] R. F. Hwang, T. Moore, T. Arumugam, V. Ramachandran, K. D. Amos, A. Rivera, B. Ji, D. B. Evans, C. D. Logsdon, *Cancer Res.* **2008**, *68*, 918.
[37] T. Stylianopoulos, J. D. Martin, V. P. Chauhan, S. R. Jain, B. Diop-Frimpong, N. Bardeesy, B. L. Smith, C. R. Ferrone, F. J. Hornicek, Y. Boucher, L. L. Munn, R. K. Jain, *Proc. Natl. Acad. Sci. USA* **2012**, *109*, 15101.
[38] B. Chaiwun, N. Sukhamwang, H. Trakultivakorn, B. Saha, L. Young, D. Tsao-Wei, W. Y. Naritoku, S. Groshen, C. R. Taylor, S. A. Imam, *Brit. J. Cancer* **2011**, *105*, 1224.
[39] M. J. Scanlan, B. K. Raj, B. Calvo, P. Garin-Chesa, M. P. Sanz-Moncasi, J. H. Healey, L. J. Old, W. J. Retting, *Proc. Natl. Acad. Sci. USA* **1994**, *91*, 5657.

Received: February 25, 2013
Revised: April 11, 2013
Published online: July 22, 2013

© 2013 Wiley-VCH Verlag GmbH & Co. KGaA, Weinheim

16136829, 2013, 14, Downloaded from https://onlinelibrary.wiley.com/doi/10.1002/smll.201300600 by Jeff Kushan - <Shibboleth>-member@gwu.edu , Wiley Online Library on [12/03/2025]. See the Terms and Conditions (https://onlinelibrary.wiley.com/terms-and-conditions) on Wiley Online Library for rules of use; OA articles are governed by the applicable Creative Commons License

Petitioner GE Healthcare – Ex. 1045, p. 2431